

The Evaluation of Tropospheric Ozone Formation in the Downwind of the South Pars Industrial Zone

Moradzadeh, M., Ashrafi, K.* and Shafiepour-Motlagh, M.

School of Environmental Engineering, College of Engineering, University of Tehran, P.O.Box 14155-6135, Tehran, Iran

Received: 09.11.2018 Accepted: 12.01.2019

ABSTRACT: Hydrocarbon Processing Industries (HPIs) emit large amounts of highly reactive hydrocarbons and Nitrogen Oxides to the atmosphere. Such simultaneous emissions of ozone precursors result in rapid and high yields ozone (O_3) formation downwind. The climate of the Middle East has been shown to be favorable for O_3 formation in summer. There are also vast activities in processing oil and gas in this region. This study aimed to investigate the influence of HPIs located in the Middle East on ozone formation. We chose the South Pars Zone (SPZ) located in the coastal area of the Persian Gulf with concentrated HPIs as a case study. To do this, after developing an emission inventory for O_3 precursors, we used OZIPR, a Lagrangian photochemical model, coupled with SAPRC-07 chemical mechanism to describe the effects of HPIs on ozone formation in the SPZ and downwind area from June to August of (2017). Results indicate that the SPZ has a far-reaching and wide-ranging impact on O_3 formation in downwind areas and an area at a distance of 300 km can be affected profoundly (Average 0.06 ppm and maximum increase 0.24 ppm). Given the large numbers of HPIs located in the Middle East, we predict that the transport of O_3 and its precursors from this region play an important role in the ozone air pollution in a much wider area and the role of these industries should be taken into account for regional and interregional ozone concentration modeling.

Keywords: Hydrocarbon Industries; Surface Ozone; HRVOCs; Photochemical Model; Middle East Climate.

INTRODUCTION

Many Asian countries are moving fast towards industrialization, which has been leading to the problem of ozone air pollution in many parts of Asia. High concentrations of ozone have been reported in many areas in Asia, especially in the Middle East. High abundance of ozone with amounts over 80 ppbv in the middle troposphere is reported by satellite observations, in situ measurements (ozone sondes) and model calculations over the

Middle East during summer (Li et al. 2001; Liu et al. 2009; Worden et al. 2009; Spohn and Rappenglück 2015). In addition, it has reported that the Persian Gulf encounters severe ozone pollution regularly (Smoydzin et al. 2012).

The Middle East is known for its enormous oil and gas reserves, large oil refineries, gas processing plants and petrochemical complexes. The processing of oil, gas and their derivatives results in remarkable emission of Volatile Organic Compounds (VOCs) and Oxides of Nitrogen (NO_x). An assessment about local air quality

* Corresponding Author Email: khashrafi@ut.ac.ir

changes over the Middle East for (2005–2014) with focusing on urban, oil refinery, oil port, and power plant targets showed that average tropospheric column levels of formaldehyde (HCHO), and glyoxal (CHOCHO) are highest over oil ports and refineries (Barkley et al. 2017). Satellite measurements confirm the high mixing ratios of tropospheric NO₂ in this area (van der A, 2008; Stavrou et al., 2008).

VOCs and NO_x are precursors that enter to the gas-phase reactions to form ground-level ozone in the presence of sun light (Haagen-Smit 1952). The absolute concentrations of NO_x and VOCs, their ratios and composition of emitted VOCs determine the rates and yields of O₃ formation (Daum et al. 2003; Lin et al. 1988; Sillman 1999). The plumes of Hydrocarbon Processing Industries (HPIs) contain simultaneous high concentrations of NO_x and reactive VOCs. These conditions lead to the fastest rate of O₃ formation and highest yields per NO_x molecule emitted (Kleinman et al. 2002; Ryerson et al. 2003; Sexton, Westberg 1983) and could be one of the main reasons of elevated concentration of ozone in the Middle East. Furthermore, Since ozone is generally regarded as a regional-scale pollutant (Auvray, Bey 2005; Wild, Akimoto 2001), it is envisaged that many areas will be affected by emission of this region. For example, results of studies in Houston showed reactive alkenes from adjacent petrochemical industries have influential role in the formation of ozone over the city (Czader et al., 2008; Allen et al., 2017; Ge et al., 2018). Also, several other studies showed that emissions from oil and natural gas activity have considerable contribution on regional O₃ production in several regions of the United States of America (Field et al., 2015; McDuffie et al., 2016, Ahmadov et al., 2015; Brantley et al., 2015; Edwards et al., 2014; Gilman et al., 2013).

This study examined an industrial zone with massive HIPs in the Middle East to explore how and in what extends these

industries effect on the ozone formation in neighboring districts. We chose the South Pars Zone (SPZ) because it encompasses the largest gas plants and petrochemical complexes in the region and even in the world and because the required data for estimating emissions were accessible.

To study the effect of the SPZ's emissions on ozone formation, in addition to NO_x and CO Emission Inventory (EI), we also prepared a fully- speciated, Reactivity-Based (RB) VOCs EI (Moradzadeh et.al. 2018). This RBEI made it possible to decide which compounds need more attention than other compounds and should be represented explicitly to the model and chemical mechanisms. Then we applied a photochemical trajectory model, OZIPR (a Research oriented version of Ozone Isopleths Plotting package), coupled with SAPRC-07 (Statewide Air Pollution Research Center) chemical mechanism to model the conditions. Trajectory models are the appropriate models to track the effects of an emission source on the downwind areas. Ozipr previously developed (Gery,Crouse 1991) and has been used to simulate photochemical pollution in many studies (da Silva et al. 2018; Alvim, et al 2018; Guarieiro et al 2017). The SAPRC photochemical mechanism has been greatly studied and validated and has been used in numerous studies around the world (Vereecken et al. 2018). Finally, with modeling the conditions of the SPZ once with and once without the emission of its HPIs, the effect of this kind of emissions was investigated.

The studies, which have assessed the ozone concentration in the Middle East to date, are mainly based on analyzing satellite and in situ measurement data (Worden et al. 2009; Liu et al. 2009; Spohn and Rappenglück,2015) or using global models. (Li et al. 2001; Lelieveld et al. 2009; Smoydzin et al. 2012).

The most of previous studies focused on the middle and upper troposphere (Li et al.

2001, Worden et al. 2009). There are just a few studies investigating the lower troposphere (Lelieveld et al. 2009, Fountoukis et al. 2018). None of them considered speciated VOCs emissions from local sources, especially Hydrocarbon Processing Industries (HPIs) that might be due to the lack of data. Thus, the influence of accumulated HPIs in the region on ozone formation has not been well explored and this is the aim of this study.

MATERIAL AND METHODS

In this study, first, we provided the required data for running the model such as emission, meteorological and boundary conditions data. Next, we ran the model for backward trajectories and evaluated the result against observed data from June to August of (2017). Then by running the model for forward trajectories once with and once without emissions of the SPZ, we assessed the impact of industrial emissions on the downwind areas. Figure 1 depicts the procedure, models and data sources used for modeling and details are described in the following text.

The SPZ is located in a narrow strip of land surrounded by the Zagros mountains and the Persian Gulf covering 140 km² as shown in Figure 2. This zone is in the vicinity of the offshore South Pars gas field, which is the largest independent gas reserve in the world. This gas field contains more than 51 trillion cubic meters of natural gas. One of the largest collections of HPIs in the world consists of ten gas processing plants with production capacity of 80,000 million cubic meters of gas and 148 million barrels of condensate annually and fourteen large petrochemical companies with the nominal capacity of 32 million tons per year have been constructed in this zone by (2017).

Ethylene, polyethylene, propylene, methanol, ammonia, granular urea, p-xylene, benzene, o-xylene, LPG are some of the main petrochemical products in the SPZ.

To prepare the required emission data for

NO_x, CO and VOCs, we needed to collect the measurement and activity data from industries located in the SPZ. The emission inventory database prepared by the Research Institute of Petroleum Industry of Iran was used for gas plants. A bottom-up emission inventory combining activity data, emission factors, modeling and Engineering calculations was prepared for petrochemical companies in collaboration with the Iranian National Petrochemical Company according to the "Emission Estimation Protocol for Petroleum Refineries-version 2.1.1" (RTI International, 2011) and "EPA's emission inventory improvement program" (Eastern Research Group, 1997). Since each VOC can significantly influence differently on ozone formation due to differences in atmospheric abundance, atmospheric reaction rates and the way in which reactions affect ozone, a reactivity-based VOCs emission inventory has been established to provide necessary input data for model and determine which compounds warrant relatively more detailed representation in modeling. The details of the preparation of this reactivity-based VOC EI has explained elsewhere (Moradzadeh et.al. 2018). There are 177 species in this inventory and propylene, ethylene, isobutylene, and formaldehyde were identified as the most important VOCs relating to ozone formation in the SPZ.

We applied OZIPR coupled with SAPRC-07 for modeling the conditions. OZIPR is a trajectory model based on a well-mixed column of air that moves with the wind. The height of the column is variable with the mixed layer but cannot expand horizontally. Various complex chemical mechanisms can be coupled with the OZIPR. Air from above the column is mixed in when the boundary layer increase and emissions from the surface enter to the column when the column passes over different emission sources (Gery, Crouse 1991). A schematic of OZIPR is shown in Figure 3.

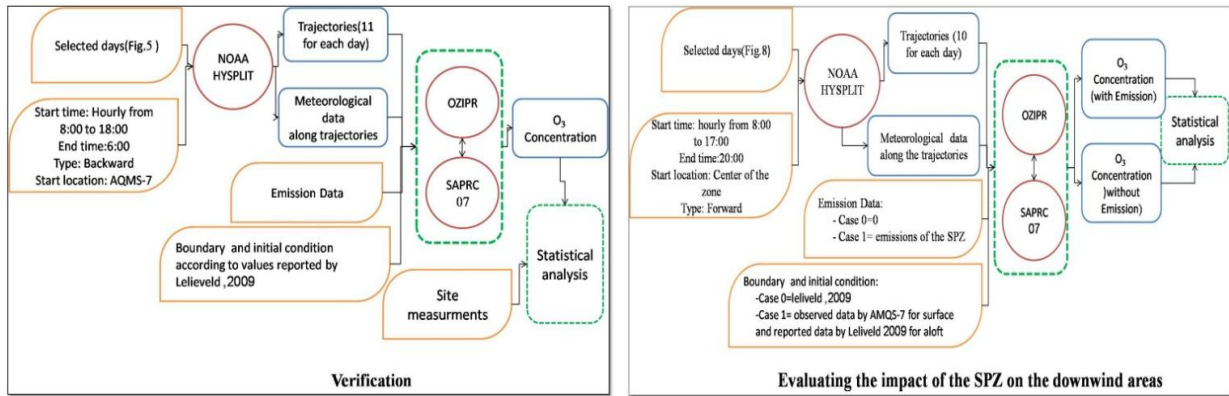


Fig. 1. The procedure and data sources used for modeling the ozone concentration in the SPZ and downwind areas



Fig. 2. The South Pars Zone on the map.

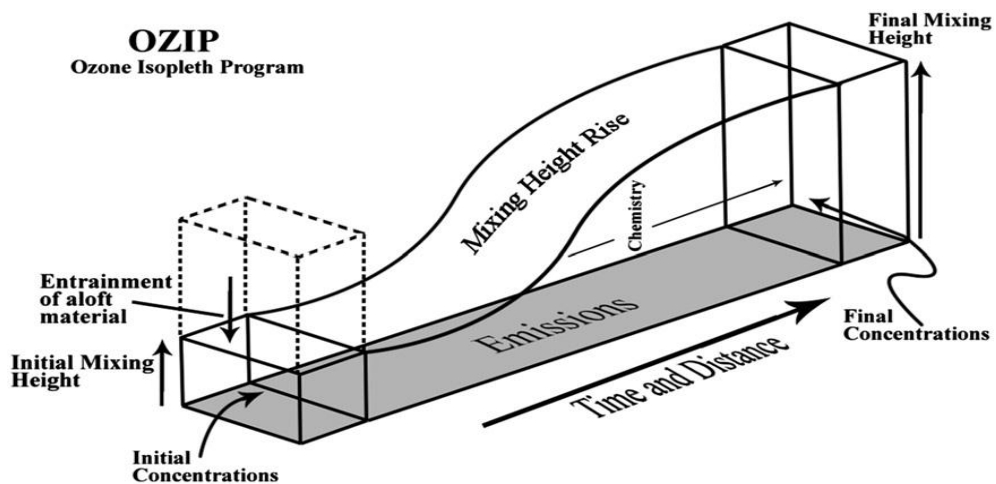


Fig. 3. Schematic of modeling in OZIPR, a well-mixed column that moves with the wind and its height change with mixing height (taken from Milt, 2009)

There are some necessary parameters must be initially set in the model as shown in Figure 3. These parameters are initial surface and aloft concentrations of the gases O₃, NO, NO₂, and CO (carbon monoxide). Hourly emission, mixing height, temperature, and relative humidity should be provided for the model along the trajectory. Other inputs such as the atmospheric VOC speciation, pressure, location, and date are needed to customize the model. Since propylene, ethylene, isobutylene, and formaldehyde had been identified as HRVOCs in the region, emission data for these compounds were given explicitly to the model.

The SAPRC07 was selected to represent chemical processes. The mechanism has separate reactions for over 700 different types of VOCs and represents approximately 300 others using the “lumped molecule” approach. In this approach, a particular organic compound or a generalized species is used to present similar organics (Dodge, 2000). The SAPRC07 mechanism has been described in detail elsewhere (Carter 2010).

The SAPRC photochemical mechanism family is used widely for regulatory and research applications (Vereecken et al. 2018). This mechanism is not as condensed as Carbon Bound (Whitten et al. 1980; Yarwood et al. 2010) and is not as detailed as the Master Chemical Mechanism (Saunders et al. 2003) and has the possibility to define some of the more influential species explicitly.

It was needed to compile emission inventory in terms of model species of the chemical mechanism chosen for the modeling (SAPRC07). A chemical speciation database managed by Carter was used for mapping chemical compounds into model species (Carter 2008).

Some field data were needed to validate the results of the model. The air quality parameters (criteria pollutants) are monitored by eight continuous air-monitoring stations (Figure 4) in the SPZ. These Air Quality

Monitoring Stations (AQMS) have been operated from May 2017 to measure the concentration of criteria pollutants (Carbon monoxide, nitrogen dioxide, ozone, particulate matter, and sulfur dioxide) in the ambient air continuously. The ozone concentration is measured by ultraviolet (UV) absorption method in these stations that is an equivalent reference method for measuring O₃ in the ambient air according to appendix P to part 50 of code of federal government of the United States regulations (interpretation of the primary and secondary national ambient air quality standards for ozone). This method is based on the absorption of ultraviolet radiation at 253.7-nm wavelength by O₃ and, the use of an ozone-specific scrubber to generate a reference air stream with only O₃ scrubbed from it.

Unfortunately, due to the short duration of operation and instability, most of AQMS did not provide valid data for the June to August of 2017 (time of this study). Among them, AQMS 7, 4 and 8 (as shown in Figure 4) provided more valid data with better time coverage. AQMS 4 is located near the emission sources and affected by them, so its data was not appropriate for comparison with the results of a well-mixed model. The AQMS 8 is often not downwind of emission sources during selected months. AQMS 7 is located near the downwind edge of the SPZ, so the data from this station was chosen as a reference.

Several days were chosen for modeling to determine whether the model can simulate the region's conditions well. The days were chosen among the ones with the valid monitoring data recorded by AQMS 7 and at least by one other station preferably AQMS 8 (just for the evaluation of data gathered by AQMS 7). On the other hand, the selected days needed to be a good representative of the summer days of the SPZ. Given these conditions, six days were selected including June 11 and 15, July 6 and 26, and August 2 and 12, (2017).



Fig. 4. A visual representation of AQMS placement in the SPZ.

After obtaining satisfactory modeling results, four days of each month (12 days) with approximately equal intervals were selected to examine the effect of the region on the downwind areas. There must be valid measurement data for these days in AQMS 7 to use as initial concentration. With these characteristics, there just were three days in August, so the ultimate numbers of selected days decreased to eleven including June 1, 11, 21, and 29, July 4, 11, 18 and 26, and August 2, 9 and 20, (2017).

OZIPR is a trajectory model and, it was necessary to calculate the trajectory of air masses for the selected days and time. Input data such as temperature, mixing height, humidity and emissions then need to be determined hourly based on this trajectory. We computed the trajectories and required meteorological data along the trajectories by the NOAA HYSPLIT (HYbrid Single Particle Lagrangian Integrated Trajectory) model. HYSPLIT computes simple air parcel trajectories using a moving frame of reference for the advection and diffusion calculations as the

air parcels move from their initial location. It has been used extensively as an atmospheric transport model in the atmospheric sciences community (Stein, 2015).

Since we needed to compare model results with measurement data in AQMS 7, we determined back trajectories from the location of AQMS 7. The back trajectories started moving at each hour (from 8:00 to 18:00 one trajectory for each hour) and ended at 6:00. Therefore, we computed 11 back trajectories per day, which each of them illustrates the movement path of an air mass before reaching AQMS 7 at a certain time. We generated these trajectories from Global Data Assimilation (GDAS) meteorological data (0.5°) and for 02/08/2017 were depicted in Figure 5 (a).

For the next step, to examine effect of the SPZ on downwind areas, we chosen forward trajectories which their start points located at the center of the SPZ and each of them started at a certain hour of day (from 8:00 to 17:00) and ended at 20:00 (10 trajectories per day) as shown in Figure 5 (b) for 20/8/2017.

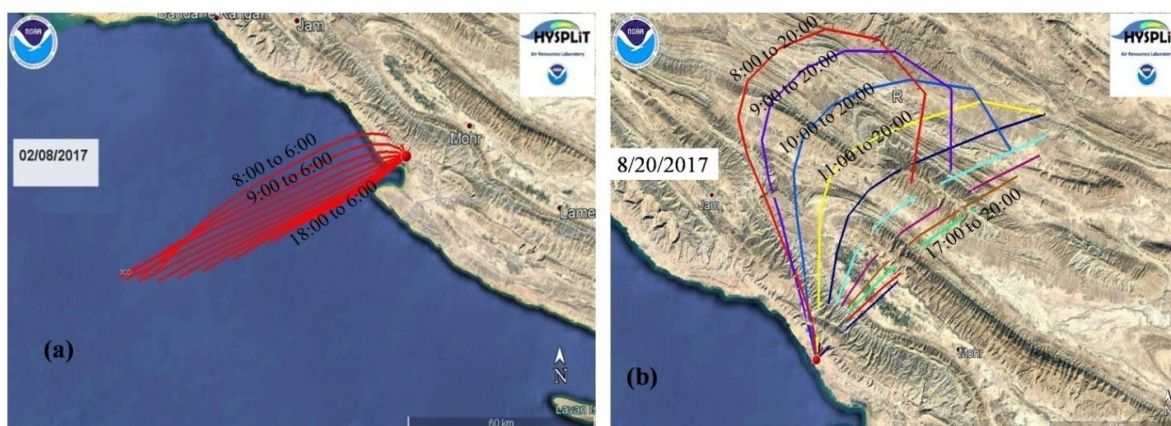


Fig. 5. (a) back trajectories from AQMS 7, starting at each hour of 02/8/2017 (from 8:00 to 18:00) to the place that air mass had been at 6:00. (b) Forward trajectories from center of the SPZ at each hour of 20/8/2017 (from 8:00 to 17:00) to the place that air mass reached at 20:00.

The next required data were the boundary conditions. The concentrations of gases in the volume of air being modeled and the aloft concentrations must be specified for the model as the initial conditions. In the present set of runs, four species including CO, O₃, VOC, and NO_x were initialized aloft. Inside the box, eight species were specified: the four aloft species, the four HRVOCs in the SPZ consist of Propylene, ethylene, isobutylene and formaldehyde (based on reactivity-based VOCs Emission Inventory) which are treated explicitly in the model. The initial concentrations of the HRVOCs were set to fixed fractions of the total VOCs, proportional to the composition of emission inventory.

For backward trajectories (used for evaluating model performance) that the air box started moving over the Persian Gulf, because of the lack of measurement data and emission sources, surface and aloft values were set to the O₃, CO, and NO_x values reported by Lelieveld et al. (2009) as shown in Table 1. There was no measured or calculated VOCs concentration for the region, therefore the VOC = 100 ppbv was considered according to the value assigned to the Houston in the study done by EPA (1999) because of the similarities between

emission sources. On the other hand, sensitivity analysis showed that the model is sensitive to aloft concentration of NO_x and, varying surface and aloft concentration of VOC to 1/2 and 2 times of the before mentioned value (0.1) may change the RMSD (Root Mean Square Deviation) between 2 to 5 ppbv. The following studies showed that this is because of the NO_x- sensitivity regime in the SPZ (results not yet published).

For forward trajectories which air mass movement started from the center of the zone (used to investigate the effect of the SPZ on downwind areas), there were two sets of runs, with emission from the SPZ (case 1) and without it (case 0). Difference between these two cases showed the influence of the SPZ on the region. For case 1, the initial surface concentrations of O₃, NO_x, and CO were determined according to the measured data by AQMs and for case 0, since the target was to eliminate all the effects of the SPZ, all the data gathered by AQMs must have been ignored. Therefore, the surface values were set according to the values calculated by Lelieveld et al., (2009) in their studies as mentioned above. Because OZIPR is not highly sensitive to deposition rates, these values were set according to the value assigned to Houston in the study done by EPA (1999).

Table 1. The surface and aloft concentrations of parameters used for initial and boundary conditions in different cases of simulation

| Simulation case | | Parameter Concentration (PPbv) | | | | |
|-----------------------------------|--------|--------------------------------|-------------------|-------------------|-------------------|------------------|
| | | O ₃ | NO _x | CO | VOCs | |
| Back trajectories ^a | | Surface. & Aloft. | 80 ^b | 1.4 ^b | 180 ^b | 100 ^c |
| | Case 0 | Surface. & Aloft. | 80 ^b | 1.4 ^b | 180 ^b | 100 ^c |
| Forward trajectories ^d | | Surface | AQMS ^e | AQMS ^e | AQMS ^e | 100 ^c |
| | Case 1 | Aloft | 80 ^b | 1.4 ^b | 180 ^b | 100 ^c |

^aAir box is over the Persian Gulf at the beginning of simulation

^b Values reported by Lelieveld et al. (2009) for the region of 25–30°N and 45–55° E

^cThe value assigned to Houston in the study done by EPA (1999)

^d Air box is over the AQMS at the beginning of simulation.

^eAir box is over the AQMS at the beginning of simulation

RESULTS AND DISCUSSION

We ran the model for 6-days and 66 trajectories to evaluate the model performance. Each trajectory specified the path of air mass from 6:00 in the morning until it reached to AQMS 7. For example, the first trajectory of each day started at 6:00 and reached AQMS 7 at 8:00, the second one started at 6:00 and ended at 9:00 over the AQMS7 and as the same way the last trajectory started at 6:00 and reached to AQMS7 at 18:00 (eleven trajectories for each day). Therefore, the last hourly value reported by OZIPR in each run was comparable with measured value in AQMS 7. Therefore totally 66 trajectories were modeled.

RMSD and R² of OZIPR outputs in relation to observations for O₃ at AQMS 7 were calculated to evaluate the model's results.

Table 2 represents the results for each day. RMSD values range from 0.0087 to 0.034 ppm. The days of June have the highest RMSD among others and, their measured values are remarkably higher than other days of this month. The total RMSD for 66 hours modeling is 0.023 ppm and, the R² is 0.76. Figure 6 shows the comparison of 66 hours modeling to observation data for O₃ concentration at AQMS 7.

Overall, the OZIPR model performed well at predicting measured concentrations at AQMS 7. Generally, the trends in both calculated and observed values are the same as evidenced by the high overall coefficient of correlation (R²= 0.78). Therefore, although in some cases the RMSD is large but acceptable for this kind of modeling (Eisele, 2009, Milt, 2009), and the overall coefficient of correlation is reasonable.

Table 2. Comparison of Simulated O₃ concentrations against the observations at Air Quality Monitoring Station (AQMS)

| surface ozone concentration (ppm) | | | | | | | | | | | | |
|-----------------------------------|-----------|-------|-----------|-------|----------|-------|-----------|-------|----------|--------|-----------|-------|
| Hour | 11/6/2017 | | 15/6/2017 | | 6/7/2017 | | 26/7/2017 | | 2/8/2017 | | 12/8/2017 | |
| | AQMS | OZIPR | AQMS | OZIPR | AQMS | OZIPR | AQMS | OZIPR | AQMS | OZIPR | AQMS | OZIPR |
| 08:00 | 0.111 | 0.105 | 0.042 | 0.107 | 0.017 | 0.049 | 0.046 | 0.044 | 0.041.5 | 0.065 | 0.046 | 0.059 |
| 09:00 | 0.131 | 0.089 | 0.072 | 0.117 | 0.039 | 0.055 | 0.071 | 0.066 | 0.060.2 | 0.095 | 0.071 | 0.061 |
| 10:00 | 0.124 | 0.112 | 0.118 | 0.158 | 0.053 | 0.066 | 0.091 | 0.088 | 0.065 | 0.097 | 0.091 | 0.066 |
| 11:00 | 0.134 | 0.127 | 0.166 | 0.162 | 0.059 | 0.075 | 0.094 | 0.089 | 0.072.9 | 0.0113 | 0.094 | 0.078 |
| 12:00 | 0.163 | 0.133 | 0.195 | 0.173 | 0.051 | 0.079 | 0.097 | 0.102 | 0.062.4 | 0.0112 | 0.097 | 0.085 |
| 13:00 | 0.170 | 0.142 | 0.158 | 0.193 | 0.057 | 0.068 | 0.071 | 0.084 | 0.059.3 | 0.0103 | 0.071 | 0.086 |
| 14:00 | 0.164 | 0.145 | 0.163 | 204 | 0.058 | 0.073 | 0.062 | 0.076 | 0.062.5 | 0.092 | 0.062 | 0.082 |
| 15:00 | 0.152 | 0.148 | 0.162 | 181 | 0.064 | 0.081 | 0.069 | 0.083 | 0.072.3 | 0.092 | 0.069 | 0.078 |
| 16:00 | 0.155 | 0.145 | 0.177 | 171 | 0.065 | 0.069 | 0.081 | 0.085 | 0.076.8 | 0.0109 | 0.081 | 0.063 |
| 17:00 | 0.153 | 0.130 | 0.179 | 164 | 0.057 | 0.036 | 0.074 | 0.073 | 0.075.9 | 0.090 | 0.074 | 0.058 |
| 18:00 | 0.140 | 0.113 | 0.167 | 133 | 0.050 | 0.029 | 0.040 | 0.052 | 0.068.9 | 0.047 | 0.040 | 0.066 |
| RMSD | 0.017 | | 0.034 | | 0.019 | | 0.008 | | 0.033 | | 0.017 | |

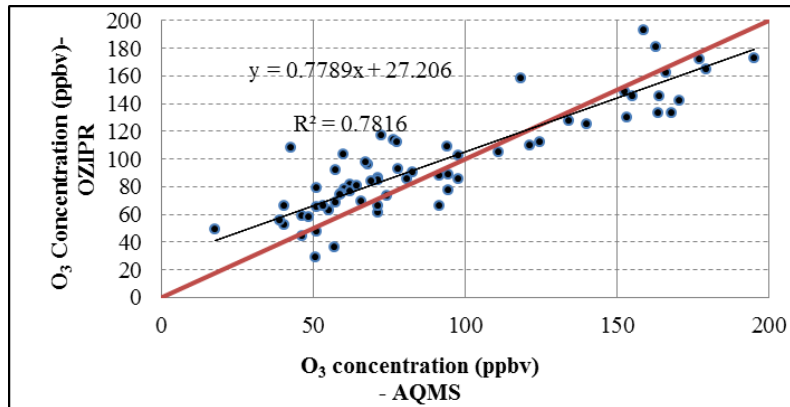


Fig. 6. Simulated O₃ concentration against observed values by AQMS 7 for 66 hours modeling from June to August of 2017, (ppbv). The red line is a criterion for error values (The higher the error value, the more point's distance from the line). The black line is the best fitting line for plotted points.

The large RMSD in some cases may be related to several factors, such as the uncertainties in the precursor emissions, the low resolution of meteorological data and simplification of the model. In preparing current inventory, normal operation of industries has been assumed whereas sudden release of VOCs is possible due to a large number of industries in the region. The OZIPR model assumes the day sunny and cloud free. The situation in the SPZ is often the same. However, there may have been cloudy days, decreasing the sunlight, which were not considered in the meteorological data used for this study.

In selected months, the predominant wind direction from 8:00 to 17:00 is from southwest to northeast. Almost Such a

pattern exists throughout summer due to the sea breeze. As mentioned before, to evaluate the effects of the SPZ on the downwind areas, forward trajectories which start hourly (8:00 to 17:00) from the center of zone were tracked by 20:00 for four days of June, July and August of 2017, once with considering emission from the SPZ (case 1) and once without it (case 0). If regardless of location, the average values are calculated for each hour per month, the hourly variation of O₃ concentration will be as shown in Figure 7. The cumulative hourly variation of ΔO₃ has been shown in Figure 8. This value (ΔO₃) is the average of differences between values for case1 and case 0 for each hour per day regardless of location.

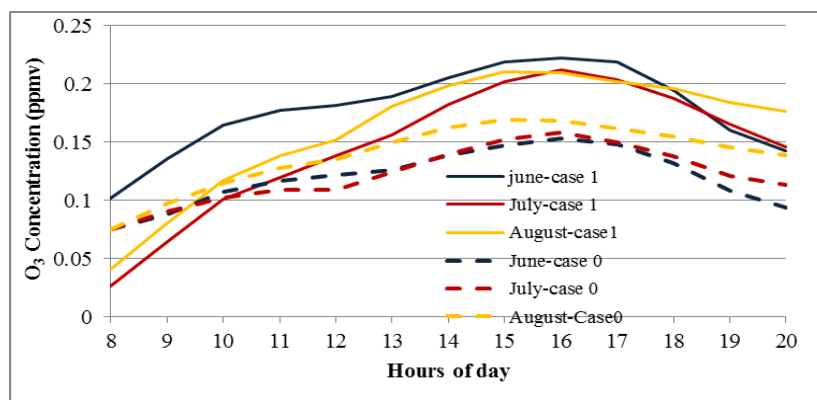


Fig. 7. Hourly variation of ozone concentration in the affected area by the SPZ for three months of 2017 for case1 (with emission) and case0 (without emission). This value is average of O₃ concentrations calculated by OZIPR for each hour, regardless of location.

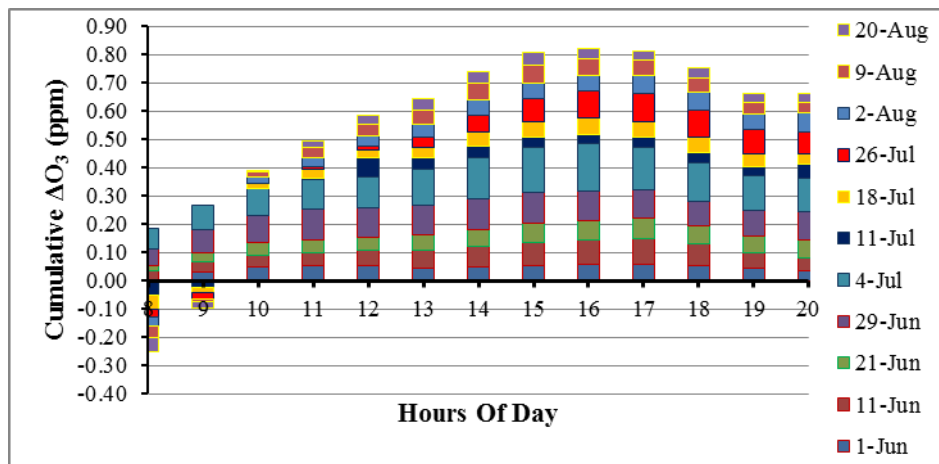


Fig. 8. Cumulative hourly variation of ozone concentration difference (ΔO_3) in the affected area by the SPZ for selected days of summer of 2017. (ΔO_3) is the difference between the values calculated by OZIPR with and without emissions from the SPZ.

Time-concentration profiles of the SPZ have the same features observed for ozone in “smoggy” ambient air. In this kind of profiles, the O_3 levels are relatively low in the early morning because there is not enough sunlight for photochemical reactions. There is another specific reason for this in Figure 7. Figure 7 shows the hourly ozone concentration in the air box as it moves from the SPZ to downwind thus in the early morning the air box is near the large emission point sources of NO. There is an important process of ozone removal associated with directly emitted NO. This process, referred to as NO_x titration, occurs because freshly emitted NO (typically, 90% or more of total NO_x emitted) reacts rapidly with O_3 to produce NO₂.

The O_3 levels increase significantly about noon near the emission sources because removal of O_3 due to NO_x titration process is small compared to the rate of ozone production which is at maximum level at noon. The process of NO_x titration can only remove maximum one O_3 per emitted NO (up to 1.5 O_3 per NO_x at night), whereas the process of ozone formation typically produces four or more O_3 per emitted NO_x (Lin et al., 1988; Liu et al., 1987; Trainer et al., 1993; Sillman et al., 1999). Downwind from emission sources, the profiles are shifted and, O_3

may peak in the afternoon as shown in Figure 7, or even after dark, depending on emissions and air shed transport phenomena. Consequently, we have the most impacts (peak of ΔO_3) in the hours of 15:00 to 17:00, as Figure 8 shows, when we had the peak of ozone concentration according to Figure 8.

It is noticeable in Figure 7 that regardless of the initial concentration of surface ozone (observed values at AQMS 7), the peak of concentration in Case 1 reaches to more than 0.2 ppm between hours 14:00 to 17:00, these values for case 0 are between 0.15-0.17 ppm at the same hours.

Although the effect of the SPZ’s emission in increasing the ozone concentration is obvious, these are unusually high amounts even for case 0.

Lelieveld et al. (2009) reported that “The Persian Gulf region is a hot spot of photochemical smog”. They calculated the average of background ozone concentration about 0.075 ppm with hourly values more than 0.08 ppm. Therefore, the results obtained in this study seem to be higher than the background ozone concentration reported by them. However, it should be considered that they report concentration of ozone near the surface over the Persian Gulf, averaged monthly

over a region of 5° latitude and 10° longitude, i.e. an area of about 0.5 million km² and calculated values in our study are hourly over the affected area from northern coast of the Persian Gulf towards the inside of Iran.

The values reach to 0.075 ppm (National Ambient Air Quality Standard (NAAQS) for ozone in Iran) in one to one and half hours after the start time of modeling and remain more than 0.15 ppm until 20:00.

The average of calculated ΔO_3 was 0.06 ppm and, the maximum was 0.24 ppm.

Increases in O₃ concentrations of at least 40 ppb in 1 h or 60 ppb in 2 h have been reported in Houston (Couzo, 2013). As mentioned before in “Introduction” section, highly reactive volatile organic compounds from petrochemical industries located in the vicinity of this city play an important role in the formation of ozone in Houston. The average ΔO_3 in the SPZ is comparable

to Houston. Additionally, the SPZ has more reactive species in its atmosphere than Houston (Moradzadeh et.al. 2018) thus even higher values are expected.

We integrated all hourly values of ΔO_3 along all the trajectories and obtained spatial and temporal Characteristics of ΔO_3 values in the SPZ. This spatial distribution has been depicted in Figure 9 for hours 15:00 to 17:00. We selected these hours because the peak concentration of O₃ occurred in this range of times almost for all trajectories (Figure 7). Figure 9 also shows the affected area at 20:00. This is the end time of the modeling period and shows the extent of the affected areas.

According to the results, a profound influence is observed in the Northeast, east and southeast of the SPZ. Plumes from the SPZ are transported slightly less than 300 km away and can cause a change in ozone concentration as much as 0.2 ppm (4 times more than NAAQS) in downwind areas.

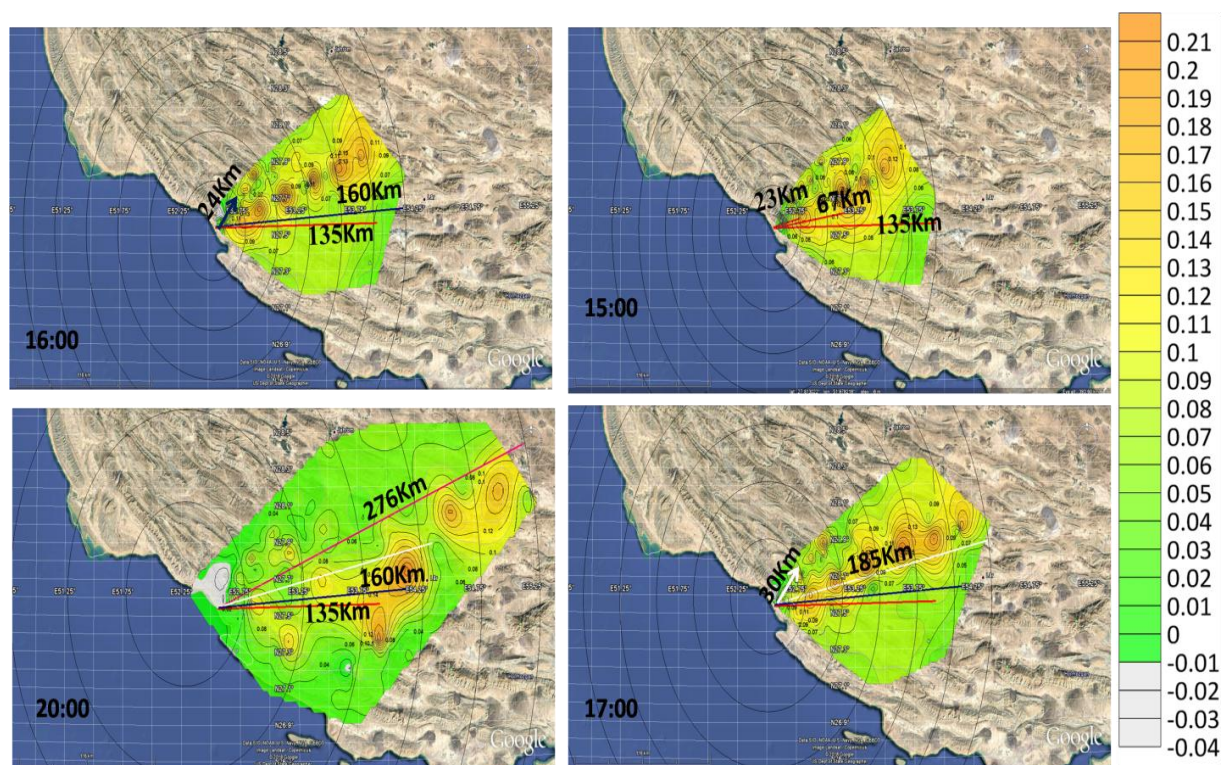


Fig. 9. Spatial distribution of ozone concentration difference (ΔO_3) in affected areas of the SPZ during 14:00 to 17:00 of days of June, July and August of 2017. (ΔO_3) is the difference between the values calculated by OZIPR with and without emissions from the SPZ.

The major impact is observed in the northeast of SPZ. Fortunately, this area is desert and without residents but other cities such as Lamerd with approximately 100,000 inhabitants is likely affected by transported plumes from the SPZ.

According to the results of an investigation done by Smoydzin et al (2012), the highest ozone concentration is observed over the Persian Gulf when the coastal anthropogenic emissions are carried with wind over the Gulf. Under these conditions, happening in the afternoon due to the sea-breeze circulation, pollution plumes are trapped in the shallow and stable marine boundary layer and therefore the ventilation is as low as possible. OZIPR is just appropriate for daytime modeling so we were not able to examine the effects of the SPZ's emissions at night or for more than one day. Therefore, further studies are needed to complete the results.

CONCLUSIONS

The SPZ encompasses many large gas refineries and petrochemical complexes. Plumes from this kind of industrial facilities routinely are characterized by coexistent elevated concentrations of NO_x and reactive VOCs. These conditions lead to the high rate of O₃ formation and highest yields per NO_x molecule emitted. Furthermore, broad regions with elevated O₃ form as the plumes travel over the down winds areas.

With appropriate customizing, OZIPR can acceptably simulate the condition. The plumes from SPZ have a far-reaching and wide-ranging impact on simulated O₃ in downwind. It can result in elevated ozone concentration in downwind areas even when the level of ozone concentration in the SPZ is not notable. Simulating ozone formation in the SPZ for 8:00 to 20:00 in summer of 2017 indicates that an area by a distance of 300 km can be affected profoundly. Given the large numbers of HPIs located in the Middle East, we predict that transported O₃ and its precursors

should result in elevated concentrations of O₃ in a broad region and the role of this industries should be taken in to account for regional and interregional ozone concentration modeling.

Because of coastal environments, it is better to discuss elevated O₃ concentrations in terms of sea breeze circulations. Therefore, it is needed to extend the duration of modeling from 12 hours to 24 or 48 hours.

It is also required to make more accurate estimations of VOCs emissions from industrial sources. In preparation of EI of the SPZ, some assumptions and simplifications were entered that modification of them can result in more accurate simulation and therefore better prediction.

ACKNOWLEDGEMENT

The contribution of National Iranian Petrochemical Co., Research Institute of Petroleum industry and Petrochemical Special Economic Zone for providing data to this study is acknowledged. Support from HSE department of Iranian Petroleum Ministry is also acknowledged.

REFERENCES

- Ahmadov, R., McKeen, S., Trainer, M., Banta, R., Brewer, A., Brown, S., Edwards, P.M., De Gouw, J.A., Frost, G.J., Gilman, J. and Helmig, D. (2015). Understanding high wintertime ozone pollution events in an oil-and natural gas-producing region of the western US. *Atmospheric Chemistry and Physics*, 15(1), pp.411-429
- Allen, D. T. (2017). Combining innovative science and policy to improve air quality in cities with refining and chemicals manufacturing: The case study of Houston, Texas, USA. *Frontiers of Chemical Science and Engineering*, 11(3), 293-304
- Alvim, D.S., Gatti, L.V., Corrêa, S.M., Chiquetto, J.B., Santos, G.M., de Souza Rossatti, C., Pretto, A., Rozante, J.R., Figueroa, S.N., Pendharkar, J. and Nobre, P.,)2018(. Determining VOCs reactivity for ozone forming potential in the megacity of São Paulo. *Aerosol and Air Quality Research*, 18(9), pp.2460-2474.
- Auvray, M., Bey, I. (2005). Long-range transport to Europe: Seasonal variations and implications for the European ozone budget. *Journal of Geophysical Research: Atmospheres* 110(D11).

- Barkley, M.P., González Abad, G., Kurosu, T.P., Spurr, R., Torbatian, S., Lerot, C. (2017). OMI air-quality monitoring over the Middle East. *Atmospheric Chemistry and Physics* 17(7), 4687-4709
- Brantley, H.L., Thoma, E.D. and Eisele, A.P., (2015.) Assessment of volatile organic compound and hazardous air pollutant emissions from oil and natural gas well pads using mobile remote and on-site direct measurements. *Journal of the Air & Waste Management Association*, 65(9), pp.1072-1082.
- Carter, W.P. (2008). Development of an improved chemical speciation database for processing emissions of volatile organic compounds for air quality models. Center for Environmental Research and Technology (CE-CERT), University of California, Riverside. <http://www.engr.ucr.edu/~carter/emitdb>.
- Carter, W.P. (2010) Development of the SAPRC-07 chemical mechanism. *Atmospheric Environment*.44(40):5324-35
- Couzo E, Jeffries HE, Vizuete W. (2013) Houston's rapid ozone increases: preconditions and geographic origins. *Environmental Chemistry*. Jun 28;10(3):260-8.
- Czader, B.H., Byun, D.W., Kim, S.T. and Carter, W.P., (2008). A study of VOC reactivity in the Houston-Galveston air mixture utilizing an extended version of SAPRC-99 chemical mechanism. *Atmospheric Environment*, 42(23), pp.5733-5742.
- da Silva, C.M., da Silva, L.L., Corrêa, S.M. and Arbilla, G.,) 2018.(A minimum set of ozone precursor volatile organic compounds in an urban environment. *Atmospheric Pollution Research*, 9(2), pp.369-378.
- Daum, P.H., Kleinman, L.I., Springston, S.R., Nunnermacker, L., Lee, Y.N., Weinstein-Lloyd, J., Zheng, J., Berkowitz, C.M. (2003). A comparative study of O₃ formation in the Houston urban and industrial plumes during the 2000 Texas Air Quality Study. *Journal of Geophysical Research: Atmospheres* 108 (D23).
- EASTERN RESEARCH GROUP, I. Air Emissions Inventory Improvement Program (EIIP) [Online]. <https://www.epa.gov/air-emissions-inventories/air-emissions-inventory-improvement-program-eiip>: EPA.)1997(.
- Edwards, P.M., Brown, S.S., Roberts, J.M., Ahmadov, R., Banta, R.M., Dubé, W.P., Field, R.A., Flynn, J.H., Gilman, J.B., Graus, M. and Helmig, D., (2014).(High winter ozone pollution from carbonyl photolysis in an oil and gas basin. *Nature*, 514 (7522), p.351.
- Eisele, A., Hannigan, M., Milford, J., Helmig, D., Milmoé, P., Thomas, G., Williams, S. and Brodin, M.,)2009(. Understanding air toxics and carbonyl pollutant sources in Boulder County, Colorado. EPA Technical Report.
- EPA.)1999(. A Simplified Approach for Estimating Secondary Production of Hazardous Air Pollutants (HAPs) Using the OZIPR Model. Office of Air Quality Planning and Standards, U.S. Environmental Protection Agency (EPA). Research Triangle Park, NC.
- Field, R.A., Soltis, J., McCarthy, M.C., Murphy, S. and Montague, D.C.,)2015(. Influence of oil and gas field operations on spatial and temporal distributions of atmospheric non-methane hydrocarbons and their effect on ozone formation in winter. *Atmospheric Chemistry and Physics*, 15(6), pp.3527-3542.
- Fountoukis, C., Ayoub, M. A., Ackermann, L., Perez-Astudillo, D., Bachour, D., Gladich, I., & Hoehn, R. D.,)2018(Vertical Ozone Concentration Profiles in the Arabian Gulf Region during Summer and Winter: Sensitivity of WRF-Chem to Planetary Boundary Layer Schemes. *Aerosol and Air Quality Research*, 18, 1183-1197.
- Ge, S., Wang, S., Xu, Q. and Ho, T.,)2018(. Ozone impact minimization through coordinated scheduling of turnaround operations from multiple olefin plants in an ozone nonattainment area. *Atmospheric Environment*, 176, pp.47-53.
- Gery, M., Crouse, R. (1991). User's guide for executing OZIPR. US Environmental Protection Agency, Atmospheric Research and Exposure Assessment Laboratory.
- Gilman, J.B., Lerner, B.M., Kuster, W.C. and De Gouw, J.A.,)2013(. Source signature of volatile organic compounds from oil and natural gas operations in northeastern Colorado. *Environmental science & technology*, 47(3), pp.1297-1305.
- Guariero, L.L.N., Amparo, K.K.S., Figueirêdo, I.S. and de Andrade, J.B., (2017). Use and Application of Photochemical Modeling to Predict the Formation of Tropospheric Ozone. *REVISTA VIRTUAL DE QUIMICA*, 9(5), pp.2082-2099.
- Kleinman, L.I., Daum, P., Imre, D., Lee, Y.N., Nunnermacker, L., Springston, S., Weinstein-Lloyd, J., Rudolph, J. (2002). Ozone production rate and hydrocarbon reactivity in 5 urban areas: A cause of high ozone concentration in Houston. *Geophysical Research Letters* 29(10).

- Lelieveld, J., Hoor, P., Jöckel, P., Pozzer, A., Hadjinicolaou, P., Cammas, J.-P., Beirle, S. (2009). Severe ozone air pollution in the Persian Gulf region. *Atmospheric Chemistry & Physics* 9(4).
- Li, Q., Jacob, D.J., Logan, J.A., Bey, I., Yantosca, R.M., Liu, H., Martin, R.V., Fiore, A.M., Field, B.D., Duncan, B.N. (2001). A tropospheric ozone maximum over the Middle East. *Geophysical Research Letters* 28(17), 3235-3238.
- Lin, X., Trainer, M., Liu, S. (1988). On the nonlinearity of the tropospheric ozone production. *Journal of Geophysical Research: Atmospheres* 93(D12), 15879-15888.
- Liu, J.J., Jones, D., Worden, J.R., Noone, D., Parrington, M., Kar, J. (2009). Analysis of the summertime buildup of tropospheric ozone abundances over the Middle East and North Africa as observed by the Tropospheric Emission Spectrometer instrument. *Journal of Geophysical Research: Atmospheres* 114(D5).
- Liu, S.C., Trainer, M., Fehsenfeld, F.C., Parrish, D.D., Williams, E.J., Fahey, D.W., Hubler, G., Murphy, P.C., 1987. Ozone production in the rural troposphere and the implications for regional and global ozone distributions. *Journal of Geophysical Research* 92, 4191D4207.
- McDuffie, E.E., Edwards, P.M., Gilman, J.B., Lerner, B.M., Dubé, W.P., Trainer, M., Wolfe, D.E., Angevine, W.M., deGouw, J., Williams, E.J. and Tevlin, A.G., (2016). Influence of oil and gas emissions on summertime ozone in the Colorado Northern Front Range. *Journal of Geophysical Research: Atmospheres*, 121(14), pp.8712-8729.
- Milt, A., Milano, A., Garivait, S. and Kamens, R.,) 2009(. Effects of 10% biofuel substitution on ground level ozone formation in Bangkok, Thailand. *Atmospheric Environment*, 43(37), pp.5962-5970.
- Moradzadeh, M., Ashrafi, K. and Shafepour, M.,)2018(. Source Apportionment Of High Reactive Volatile Organic Compounds In a Region With The Massive Hydrocarbon Processing Industries. *Environmental Energy and Economic Research*, 2(1), pp.37-49.
- RTIINTERNATIONAL (2011). Emissions Estimation Protocol for Petroleum Refineries.
- Ryerson, T., Trainer, M., Angevine, W., Brock, C., Dissly, R., Fehsenfeld, F., Frost, G., Goldan, P., Holloway, J., Hübler, G. (2003). Effect of petrochemical industrial emissions of reactive alkenes and NO_x on tropospheric ozone formation in Houston, Texas. *Journal of Geophysical Research: Atmospheres* 108(D8).
- Saunders, S.M., Jenkin, M.E., Derwent, R., Pilling, M.: Protocol for the development of the Master Chemical Mechanism, MCM v3 (Part A) (2003). tropospheric degradation of non-aromatic volatile organic compounds. *Atmospheric Chemistry and Physics* 3(1), 161-180.
- Sexton, K., Westberg, H. (1983). Photochemical ozone formation from petroleum refinery emissions. *Atmospheric Environment* (1967) 17(3), 467-475.
- Sillman, S. (1999). The relation between ozone, NO_x and hydrocarbons in urban and polluted rural environments. *Atmospheric Environment* 33(12), 1821-1845.
- Smoydzin, L., Fnais, M., Lelieveld, J. (2012). Ozone pollution over the Arabian Gulf--role of meteorological conditions. *Atmospheric Chemistry & Physics Discussions* 12(2).
- Spoehn, T.K. and Rappenglück, B., (2015). Tracking potential sources of peak ozone concentrations in the upper troposphere over the Arabian Gulf region. *Atmos. Environ.* 101: 257–269.
- Stavrakou, T., Müller, J.F., Boersma, K.F., De Smedt, I. and Van Der A, R.J., (2008(.Assessing the distribution and growth rates of NO_x emission sources by inverting a 10-year record of NO₂ satellite columns. *Geophysical Research Letters*, 35(10).
- Stein AF, Draxler RR, Rolph GD, Stunder BJ, Cohen MD, Ngan F. (2015). NOAA's HYSPLIT atmospheric transport and dispersion modeling system. *Bulletin of the American Meteorological Society*. Dec;96(12):2059-77.
- Trainer, M., Parrish, D.D., Buhr, M.P., Norton, R.B., Fehsenfeld, F.C., Anlauf, K.G., Bottenheim, J.W., Tang, Y.Z., Wiebe, H.A., Roberts, J.M., Tanner, R.L., Newman, L., Bowersox, V.C., Maughner, J.M., Olszyna, K.J., Rodgers, M.O., Wang, T., Berresheim, H., Demerjian, K., (1993). Correlation of ozone with NO_y in photochemically aged air. *Journal of Geophysical Research* 98, 2917D2926.
- Van Der A, R.J., Eskes, H.J., Boersma, K.F., Van Noije, T.P.C., Van Roozendael, M., De Smedt, I., Peters, D.H.M.U. and Meijer, E.W.,)2008(. Trends, seasonal variability and dominant NO_x source derived from a ten year record of NO₂ measured from space. *Journal of Geophysical Research: Atmospheres*, 113(D4).
- Vereecken, L., Aumont, B., Barnes, I., Bozzelli, J.W., Goldman, M.J., Green, W.H., Madronich, S., McGillen, M.R., Mellouki, A., Orlando, J.J. and Picquet-Varrault, B., (2018(. Perspective on Mechanism Development and Structure-Activity Relationships for Gas-Phase Atmospheric Chemistry. *International Journal of Chemical Kinetics*, 50(6), pp.435-469.

Whitten, G.Z., Hogo, H., Killus, J.P. (1980). The carbon-bond mechanism: a condensed kinetic mechanism for photochemical smog. *Environmental science & technology* 14(6), 690-700.

Wild, O., Akimoto, H. (2001). Intercontinental transport of ozone and its precursors in a three-dimensional global CTM. *Journal of Geophysical Research: Atmospheres* 106(D21), 27729-27744.

Worden, J., Jones, D., Liu, J., Parrington, M., Bowman, K., Stajner, I., Beer, R., Jiang, J., Thouret,

V., Kulawik, S. (2009). Observed vertical distribution of tropospheric ozone during the Asian summertime monsoon. *Journal of Geophysical Research: Atmospheres* 114(D13).

Yarwood, G., Jung, J., Whitten, G.Z., Heo, G., Mellberg, J., Estes, M. (2010). Updates to the Carbon Bond mechanism for version 6 (CB6). In: 2010 CMAS Conference, Chapel Hill, NC. October. (http://www.cmascenter.org/conference/2010/abstracts/emery_updates_carbon_2010.pdf).

